ANALYSIS OF JET COMPONENT PARAMETERS OF SUPERLUMINAL SOURCES SELECTED BASED ON SIZE AND DISTANCE FROM THE CORE

ANEKWE FRANCES AND ONUCHUKWU CHIKA
Department of Industrial Physics, Chukwuemeka Odumegwu Ojukwu University, Uli, Anambra State, Nigeria

ABSTRACT
We studied comparatively the observed jet components properties (luminosity,P, projected distance, D_p, component size, a, apparent speed, β_a and absolute difference between the weighted mean position angle and the proper motion position angle, $|P.A. - \varphi|$) of superluminal sources selected based on size and distance from the core. We formed jet component subsamples of biggest, (BG), smallest, (SM), farthest, (FAR), and the innermost, (INN) components. The log of luminosity distribution plot indicate a log normal distribution for all jet component subsamples. The SM jet component subsample seem to have higher average luminosity than the BG, FAR, and INN component subsamples, the BG and FAR subsamples are the dimmest. The log of projected distance distribution plot, also showed log normal distribution for the SM and INN component subsamples. The distribution plot of the log of apparent speed showed a log normal distribution for all BG/SM and FAR/INN component subsamples. The log distribution plot of the size (a) for BG and INN component subsamples seem to show a log normal distribution pattern, the SM components are totally different following a one tailed distribution, and the FAR indicates no known pattern distrubtion, though at higher values of a, both FAR and INN slow similar distribution.

Keyword: **Galaxies – Miscellenous; Method – Data Analyis; Jets.**

1. INTRODUCTION

Active Galactic Nuclei (AGN) is a generic term used to include all galaxies with extra ordinary activities in the nuclei. The nuclei of these galaxies are known to produce very high luminosities in a concentrated volume through the accretion of matter onto a central object. AGNs are special high-energy laboratories and can serve as our principal probe of the Universe on large scales. Our understanding of them is important in studying the formation/evolution of the galaxies, which are the building block of the Universe.

The AGN model of Blandford&Königl (1979) is the generally accepted basic model of AGN. It considers that at the center of the galaxy there is a supermassive black hole, surrounded by an accretion disk. The high luminosity originated at the central region of the system, where the black hole accretes matter from the disk. Other than the matter coming from the disk, the black hole ejects matter at very high speeds forming two opposite, powerful jets. The process of jet launching is not yet well understood. The power of the black hole makes that outgoing matter travels with a highly relativistic speed. Strong optical and UV emission lines are produced in clouds of gas moving rapidly in the potential of the black hole (De Young, 2002)

Outflow of energetic particles (refer to as jet) occur along the poles of the disk or torus, escaping and forming collimated radio-emitting jets (the plasma in the jets, at least on the smallest scales, streams out at very high velocities, beaming radiations relativistically in the forward direction), and sometimes giant radio sources when the host galaxy is elliptical (Urry&Padovani, 1995). Observing these jets of AGN at pc scale with Very Long Baseline Interferometers have shown that these jets are not continuous but forms blob of radiationemitting plasma called jet

components. The study of the evolution of these jet components is important in the understanding the kinematics and evolution dynamics of AGN.

In this paper, using observed jet parameters, we compare the characteristics of jet components properties selected based on biggest/smallest jet components and the innermost and outermost jet components with respect to the stationary core.

2. DATA DESCRIPTION

The sample used for this analysis was taken from Piner*et al.,* (2007). The sample contains 2579 Gaussian components of 77 sources with observed redshift (z), jet component size (a) in miliarcsec (mas), jet component distance from an assumed core (D) also in mas, component flux density (S) in Jansky (Jy) and apparent superluminal speed (β_a). From the optical class identifications by Veron-Cetty&Veron (2010), there are 56 sources which were classified as quasars, 7 as BL Lac objects, 4 as galaxies, and 1 was unidentified. We selected only the quasars for our analysis due to the low number statistics of other classes of radio sources. For each source, we selected all the components with positive apparent speed, since simple relativistic beaming theory of AGN assumed that the jet component motion can be simplified as ballistic motion (Kellermann*et al.,* 2004, Piner*et al.,* 2007, 2012; Onuchukwu&Ubachukwu, 2013). The final sample consists of 64 sources, with most of the sources having more than one component. Each jet component had at least five epochs of observations (Piner*et al.,* 2007).

We formed subsamples based on luminosity (brightest (BR) and dimmest (DM) subsamples) and observed distance from the assumed core (Farthest (FAR) and Innermost (INN) subsamples). Sources with only one component are represented in the four different subsamples by that component. For each jet components there are at least five epochs of observations (Piner*et al.,* 2007). We obtained the average values of the parameters - a, D and Swhich we used in the analysis (the redshift z is the same for different jet components of the same source).We converted a into the jet component size (R) in the frame of the observer, D into projected distance D_P in pc and S into luminosity P in WHz^{-1} using the expression found in Leahy *et al.*, (1991)

3. METHOD OF ANALYSES

We employed descriptive statistics which include histogram plots and central tendency values, in the study of the various subsamples of the jet component parameters of superluminal sources. This will enabled us to highlight the possible differences and similarities in the parameters of these various subsamples of jet components (BG/SM and FAR/INN)

4. ANALYSES AND RESULTS

In Figure 1, we display the distribution plot of the $\log P$of BG, SM, FAR and INN subsample. The distribution seems to be log normal for all the subsamples. The BG component subsample peaked at a lower value of (10^{24} – 10^{25}) WHz^{-1} while the SM components peaked at a higher value of about 10^{25} – $10^{26}WHz^{-1}$ and the INN subsample peaked at $10^{26\text{-}27}WHz^{-1}$ higher than the SM subsamples. The plot also showed that at lower luminosity, (< 10^{23}) SM and FAR component subsamples are not observed. SM component subsample seem to have higher average luminosity than the BG, FAR, and INN component subsamples.

Figure 2 is the distribution plot of the log of the projected distance for BG/SM and FAR/INN component subsamples. The plot indicates log normal distribution for the SM and INN component subsamples, with both the INN and SM component subsamples found closer to the core. The BG components are at greater distance from the core and perhaps due to expansion,

fades away and can no longer be detected at very large distances away from the core, see the sudden drop at distances greater than $10^{1.7\text{-}1.9}$ ~ 50.12 – 79.43 pc, while that of the farthest component has no pattern. The innermost components peaks at $10^{0.3\text{-}0.5}$~ 2.00 – 3.16 pc, smallest component subsamples peaked at $10^{0.5\text{-}0.7}$ ~ 3.16 –5.01 (pc) while the farthest and biggest component subsamples both peaked at a higher value of $10^{0.9\text{-}1.1}$ ~ 7.94 – 12.60 (pc).

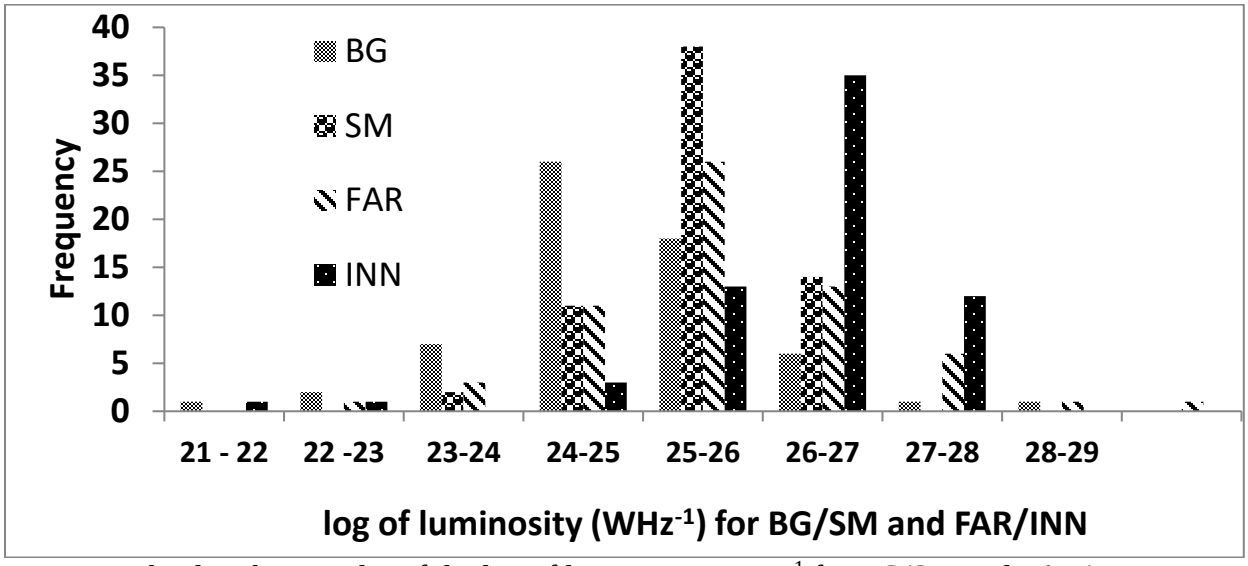

Figure 1: The distribution plot of the log of luminosity, WHz^{-1} for BG/SM and FAR/INN subsamples.

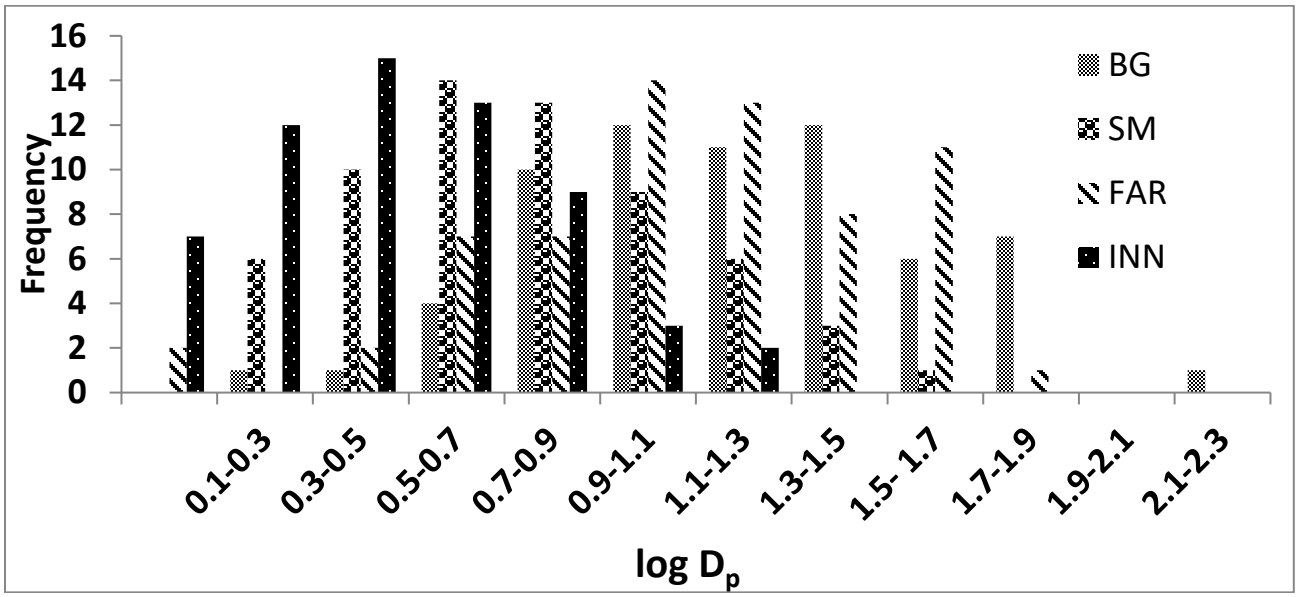

Figure 2: The distribution plot of the log of the projected distance for the BG/SM and FAR/INN subsamples

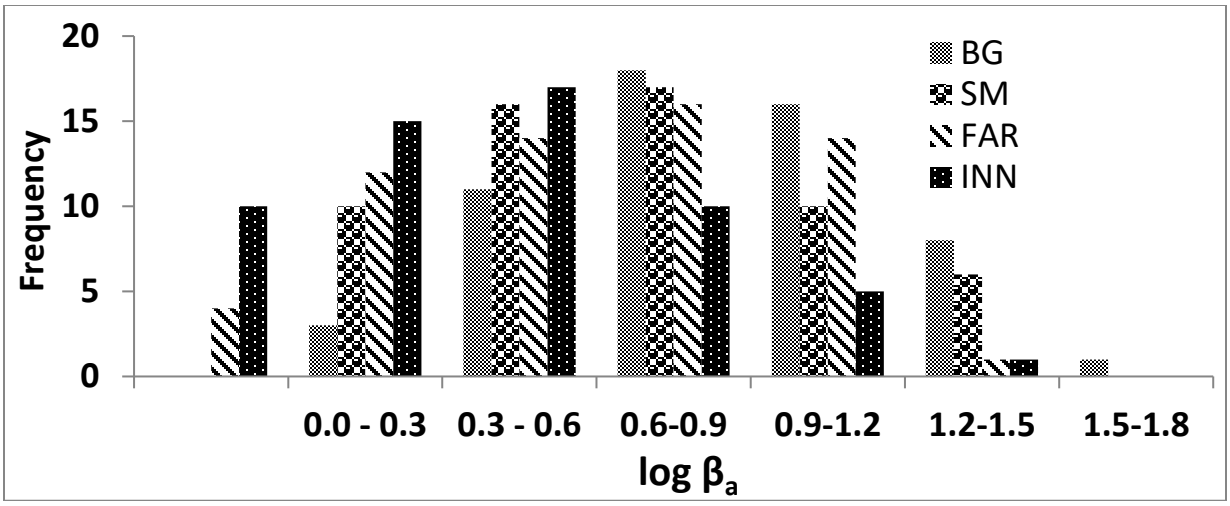

Figure 3: The distribution plot of log of apparent speed for the BG/SM and FAR/INN component subsamples.

In Figure 3 is displayed the distribution plot of the log of apparent speed for the biggest, smallest, farthest and innermost component subsamples. The plot showed a log normal distribution for all BG/SM and FAR/INN component subsamples. The BG, SM and FAR all peaked at $10^{0.6\text{-}0.9}$ ~ 3.98 – 7.94 *c*, (where c is the speed of light), while INN subsample peaked at $10^{0.3\text{-}0.6}$ ~ 2.00 – 3.98 c. The speed distribution for the BG/SM and FAR/INN components being similar indicates constant expansion speed, as the components moves away from the core.

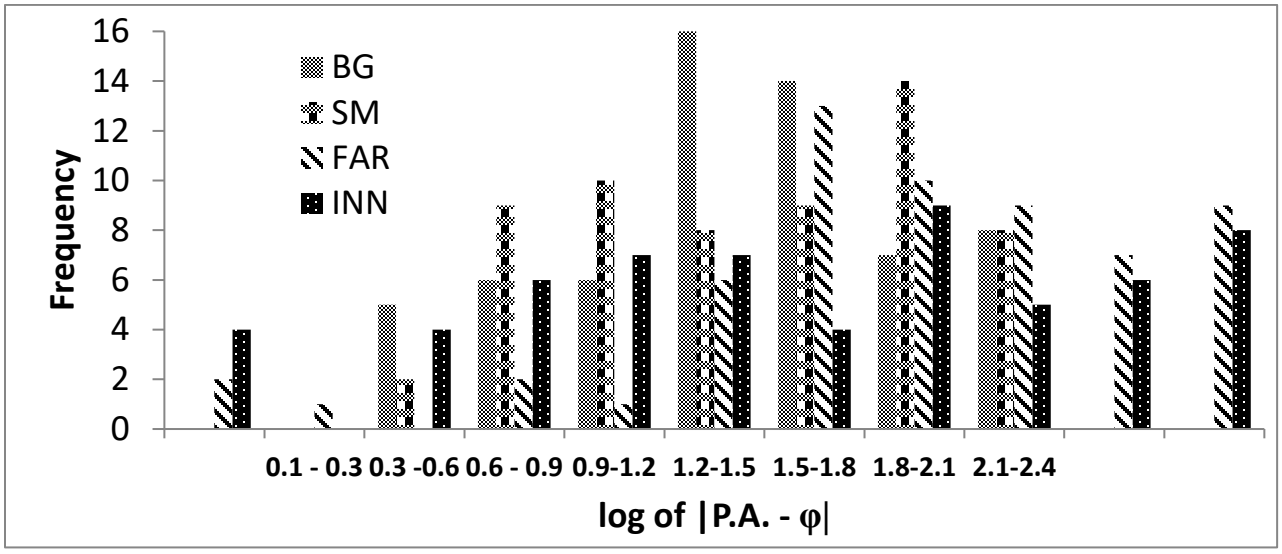

Figure 4: The distribution of the plot of log of |P.A. – ϕ| for BG/SM and FAR/INN component subsamples.

In Figure 4, we showed the distribution plot of the log |P.A. – ϕ| for the BG, SM, FAR and INN component subsamples. For the BG components, the |P.A. – φ| showed steady frequency between |P.A. – φ| $10^{0.3\text{-}1.2}$ ~ 2.00 deg to 15.85 deg. The BG components peaked at $10^{1.2\text{-}1.5}$ ~ 15.85 – 31.62 (deg) while the SM and INN component subsamples peaked at $10^{1.8\text{-}2.1}$ ~ 63.10–125.90 (deg), this is an evidence of ballistic motion within the inner part of the jet.

Where as the FARcomponent subsample peaked at $10^{1.5\text{-}1.8}$~31.52 – 63.10 deg. The plot showed no sequence/pattern for both FAR and INN components, this may indicate non-ballistic motion of the component subsample as they evolve away from the point of ejection, always assumed for jets propagation in AGN. Since the position angle is not randomized, implying no preferred direction in these jet motion.

In the Figure 5, we present the log of the distribution of the size of the components for the BG, SM, FAR, and INN component subsamples. The BG and INN component subsamples seem to show a log normal distribution pattern, the SM components are totally different following a one tailed distribution, and the FAR indicates no known pattern distrubtion, though at higher values of a i.e. $10^{1.2\text{-}1.35}$ ~ 15.84 – 22.39 pc, both FAR and INN slow similar distribution, note that for the BG components, the size frequency increased from a minimum to a maximum and then decreases until the largest size $10^{1.3\text{-}1.5}$ ~ 19.95 – 31.62 pc. The plot also show that INN/SM component subsamples peaked at $10^{0.15\text{-}0.30}$ ~1.41 – 2.00 pc, BG peaked at $10^{0.6\text{-}0.75}$~ 3.98 – 5.62 pc while the FAR components peaked at $10^{0.30\text{-}.45}$ ~ 2.00 – 2.82 pc respectively.

The averages values shown in the Table 1 indicate that BG has the lowest luminosity value than SM, INN and FAR subsamples. Interestingly, SM and INN have the same value of apparent speed and so do BG and FAR subsamples, also the FAR subsamples are bigger in size and hence the brightest. The innermost subsamples are the dimmest and it also has the least |P.A. – φ| value. The INN is very close to the core.

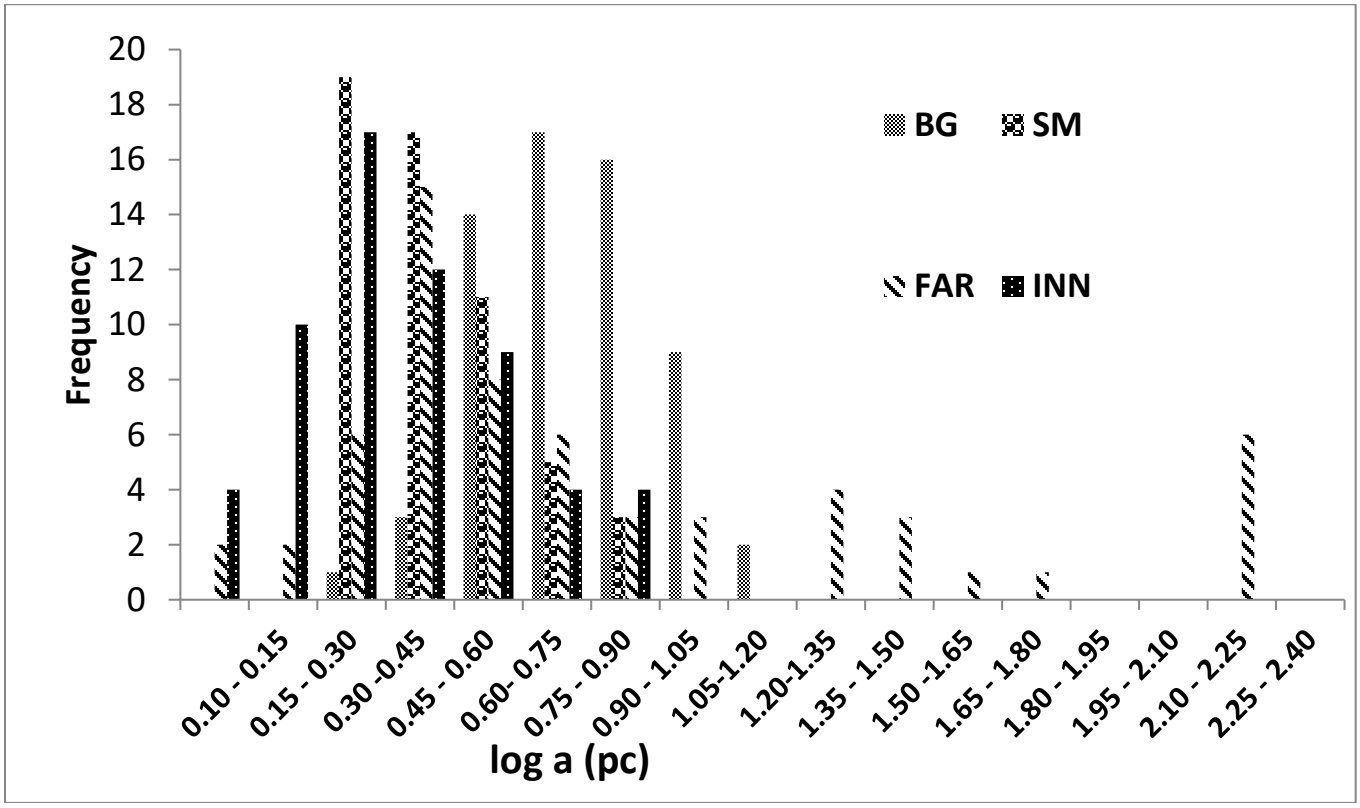

Figure 5: The distribution of the plot of log of a for BG/SM and FAR/INN component subsamples.

Table 1: Mean values for the biggest/smallest and the farthest/innermost component subsamples.

Parameter	**Mean**			
	BG	**SM**	**INN**	**FAR**
log P	**24.68**	**25.50**	**25.25**	**24.69**
log a	**0.81**	**0.31**	**0.35**	**0.84**
log D_p	**1.20**	**0.67**	**0.60**	**1.29**
log β_a	**0.73**	**0.52**	**0.52**	**0.73**
log |P.A. – ϕ|	**1.43**	**1.38**	**1.28**	**1.54**

5. CONCLUSION

We analyzed the superluminal jet components properties of AGN using jet component parameters which include $(P, D_p,\ a, \beta_a, |P.A. - \varphi|)$ for the jet components subsamples selected based size and distance from an assumed stationary core – biggest, smallest, outermost and innermost (BG, SM, FAR, and INN). The log of luminosity distribution plot indicate a log normal distribution for all component subsamples of BG/SM and FAR/INN.

Our result indicates that the smallest jet components are also the innermost jet components and brighter, while the biggest jet components are the farthest from the core and dimmer. This could be explained using the modified King density profile (King 1972), given as $\rho_r \propto \left[\left(1 + \left(\frac{D}{D_o}\right)^2\right)\right]$, where D_o is some assumed inner distance from the core. Within the inner regions of the galaxies, density is high, preventing the jet components from increasing in size, while increased interaction of the plasma with surrounding materials leads to increased luminosity. Within the outer regions of the galaxies, density is lower, thus the jets can increase to arbitrary sizes, interact less with surrounding media and thus lower luminosity. We also expect the apparent speed of the outermost components to be higher than those of the innermost/smallest components. This will be investigated in another paper.

In general, our results are in agreement with what was observed in Onuchukwu&Ubachukwu (2012). In their study on the Lorentz factors of superluminal sources, they showed that for the sample selection based on the brightest components, the apparent speed, component size, and component distance from the assumed stationary core, have less average Lorentz factor than those of the sample selected based on fastest components, but has brighter apparent luminosity. These components have smaller and apparently brighter components, but if they move without obstruction, they should also, on average, have higher apparent speed. This is an indication that their apparent luminosity might be more of a projection effect/motion through bends than being relativistically Doppler boosted. Thus, the Lorentz factor calculated based on brightest components for a given sample will most likely represent the lower limit of the bulk expansion speed, and the upper limit of the viewing angle, while that estimated from the fastest components will represent the most probable values (Gopal-Krishna *et al.,* 2006; Wiita*et al.,* 2008; Marshall *et al.,* 2011; Hovatta*et al.,* 2009).

REFERENCES

Blandford, R.D., Königl, A. (1979). 'Relativistic Jets as Compact Radio Sources',
*Astrophysical Journal, **232, 34.***

De Young, D. S. (2002). 'The Physics of Extragalactic Radio Sources' *the University of*

Cambridge press: Chicago & London, p22.

Gopal –Krishna, Wiita, P. J., Dhurde, S. (2006). 'Bulk Motion of Ultrarelativistic Conical Blazar Jets', *Monthly Notices of Astronomical Society, **369, 1287G***

Hovatta, T., Nieppola, E., Tornikoski, M., Voltaoja, E., Aller, M. F., and Aller, H. D. (2008). 'Long-term radio variability of AGN: flare characteristics', *Astronomy & Astrophysics, **485, 51***

Kellermann, K. I., Lister, M. L., Homan, D. C., Vermeulen, R. C., Cohen, M. H., Kaddler, M., Zensus, J.A., and Kovalev, Y.Y. (2004). 'sub-Milliarcsecond Imaging of Quasars and Active Galactic Nuclei. III. Kinematics of Parsec-scale Radio Jets', Astrophysical Journal, **607, 539.**

King, I. R. (1972). 'Density Data and Emission Measure for a Model of the Coma Cluster', *Astrophysical Journal, Vol. **174, L123.***

Leahy, J. P., and Perley, R. A. (1991). 'VLA images of 23 Extragalactic Radio Sources', Astrophysical Journal, **102, 537L**

Marshall, H. L., Miller, B. P., Davis, D. S., Perlman, E. S, Wise, M., Canizares, C. R., and Harris, D. E. (2002). 'A high Resolution X-ray Image of the Jet in M87', Astrophysical Journal, 564, 683.

Onuchukwu, C.C., and Ubachukwu, A.A., (2013). 'On The Lorentz Factor of Superluminal Sources', *Research in Astronomy and Astrophysics, **Vol. 13, No.5, 509.***

Piner, B. G., Pushkarev, A. B., Kovalev, Y. Y., Marvin, C. J., Arenson, J. G., Charlot, P., Fey, A. L., Collioud, A., and Voitsik, P. A. (2007). 'Relativistic Jets inthe Radio Reference Frame Image Database. II. Blazar Jet Accelerations fromthe First 10 Years of Data (1994–2003)', *Astrophysical Journal,* **758, 84**

Urry, P., Paolo, Padovani (1995). 'Unified schemes for radio loud AGN' *Publications of the Astronomical Society of the Pacific **107, 845.***

Veron-Cetty, M. P., and Veron, P. (2010). 'Active Galactic Nuclei (13th Ed.)', *Astronomy and Astrophysics, **518, A10***

Wiita, P. J., Gopal-Krishna, Dhurde, S., and Sircar, P. (2008). 'Effects of Opening Angle and Velocity Structure on Blazar Parameter', *Astrophysical Conference, **386, 522.***